CDF note 7862

# Measurement of the Ratio of Branching Fractions $Br(B_s \to D_s\pi)/Br(B^0 \to D^+\pi)$


The CDF Collaboration
*URL http://www-cdf.fnal.gov*



(Dated: October 18, 2005)



The measurement of $B_s$ mixing is one of the most important analyzes for the Run II $B$ physics program. The sensitivity of the measurement to the frequency of $B_s$ oscillations strongly depends on the number of reconstructed $B_s$ mesons. In this note we reconstruct $B_s$ in its decay to $D_s^-\pi$ with $D_s^- \to \phi\pi^-$ and measure yield compared to $B^0 \to D^-\pi(D^- \to K\pi\pi)$

After correcting for the relative trigger and reconstruction efficiencies we measure

$$\frac{f_s}{f_d} \cdot \frac{Br(B_s \to D_s\pi)}{Br(B^0 \to D^-\pi)} = 0.263 \pm 0.017(stat) \pm 0.008(syst) \pm 0.039$$

Using the PDG 2005 value for $f_s/f_d = 0.259 \pm 0.038$ we obtain

$$\frac{Br(B_s \to D_s\pi)}{Br(B^0 \to D^+\pi)} = 1.02 \pm 0.07(stat) \pm 0.03(syst) \pm 0.15(BR) \pm 0.15(PR)$$

## I. ANALYSIS DESCRIPTION

This note describes a measurement of relative branching ratio of $B_s \to D_s\pi$ to $B^0 \to D\pi$ in $\bar{p}p$ collisions at $\sqrt{s} = 1.96$ TeV with the CDF detector at the Fermilab Tevatron. The CDF detector is described in detail in [1].

For the measurement of the relative branching ratio we need to extract the total efficiency, $\epsilon_{\rm tot}$, which is here subdivided into trigger and reconstruction efficiency. The relative branching ratio is then given by

$$\frac{\sigma_{B_s} \cdot Br(B_s \to D_s\pi)}{\sigma_{B^0} \cdot Br(B^0 \to D\pi)} = \frac{\epsilon_{tot}(B^0)}{\epsilon_{tot}(B_s)} \cdot \frac{Br(D)}{Br(D_s)} \cdot \frac{N_{B_s}}{N_{B^0}}. \tag{1}$$

In principle, $B^0$ and $B_s$ are two separate samples which have different properties. Further input quantities are the numbers of events, $N_B$, the production cross section for the particular $B$ species, $\sigma_B$, and the subsequent $D$ branching ratios, $Br(D)$. The number of events are extracted from the data, while the efficiencies are extracted from the Monte Carlo simulation. Branching ratios and cross sections are obtained from the PDG [2]. The cross section ratio is therefore reduced to the ratio of production fractions, $f_s/f_d$.

## II. DATA SAMPLE & EVENT SELECTION.

We used $355pb^{-1}$ of CDF two track trigger data to measure the ratio of branching fractions. Cut optimization was done maximizing the significance of the scaled Monte Carlo signal over combinatorial background. The signal region was blinded. Final cuts are listed in the blessed tables below.

CDF two track trigger is divided into three branches with the following requirements on the pair of tracks:

- `B_CHARM`: opposite charge between the two tracks, each track $p_T > 2.0$ GeV, linear sum $p_T > 5.5$ GeV, $0.034906585 < \Delta\phi < 1.5707963$ and $L_{xy} > 0.02$ cm
- `LOWPT`: no opposite charge requirement, each track $p_T > 2.0$ GeV, no additional linear $p_T$ sum requirement and $L_{xy} > 0.02$ cm
- `B_CHARM_HIGHPT`: opposite charge between the two tracks, each track $p_T > 2.5$ GeV, linear sum $p_T > 6.5$ GeV, $0.034906585 < \Delta\phi < 1.5707963$ and $L_{xy} > 0.02$ cm

During normal running conditions all of these triggers are being prescaled. As the luminosity goes down during the store the values of effective prescales change to utilize the full bandwidth of the trigger system.

The Figure 1 shows sketch of the set of the selection requirements of the trigger (phase space) versus triggers effective prescale. The trigger which is most strongly prescaled is the trigger with the loosest selection requirements (`LOWPT`). For this measurement the `B_CHARM` and `LOWPT` part of the trigger was used.

## III. MONTE CARLO SIMULATION.

We generated realistic Monte Carlo with run by run weighted luminosity and prescale. We used Monte Carlo to optimize selection cuts, to describe fitting shape for signal along with partially reconstructed decays and to study analysis efficiency. `BGenerator` was used to produce $B$-mesons and `EvtGen` [4] to decay them. Default $B$-meson transverse momentum spectrum used by `BGenerator` was corrected to agree with $B$-hadron spectrum measured at CDF [3]. `BGenerator` is a commonly used program to create $B$ mesons. It is based on NLO calculations [5] and the fragmentation is implemented using the Peterson fragmentation function [6]. `BGenerator` only produces $B$ mesons, no fragmentation products or proton remnants are present.

## IV. EXTRACTION OF SIGNAL YIELDS.

Fitting shapes for signal and partially reconstructed decays were taken from Monte Carlo with signal width corrected using input from data. The final fit was done fixing shapes for partially reconstructed decays. Their relative normalization were allowed to float as well as mass of the signal and parameters describing combinatorial background. The relative to the signal normalizations of various backgrounds directly under the peak were fixed using Monte Carlo information.

## V. SYSTEMATICS.

The systematic uncertainties are listed in the table III.$B$ $p_T$ spectrum uncertainty is due to the fact that the ratio of Monte Carlo efficiencies is different when using default Monte Carlo spectrum and measured one. $\phi^0$ mass cut uncertainty is due to the fact that $\phi^0$ mass cut is present for the one mode and not present for the other. Lifetime uncertainties are due the dependence of efficiencies on the value of lifetimes. $B_s$ fitting uncertainty is mostly because of the unknown Branching fractions in $B_s$ sector and unceratainty of the normalizations of the backgrounds under the signal peak. $B^0$ fitting uncertainty comes from fit instability with respect to fixed parameters.

## VI. BLESSED RESULT.

We present a measurement of the branching ratio $f_s/f_d \cdot Br(B_s \to D_s\pi)/Br(B^0 \to D^+\pi)$. Our result from the combined `B_CHARM` and `LOWPT` trigger data is:

$$\frac{f_s}{f_d} \cdot \frac{Br(B_s \to D_s\pi)}{Br(B^0 \to D^-\pi)} = 0.263 \pm 0.017(stat) \pm 0.008(syst) \tag{2}$$

Using the PDG 2005 value for $f_s/f_d = 0.259 \pm 0.038$ [2] we obtain the following ratio of branching ratios

$$\frac{Br(B_s \to D_s\pi)}{Br(B^0 \to D^+\pi)} = 1.02 \pm 0.07(stat) \pm 0.03(syst) \pm 0.15(BR) \pm 0.15(PR)$$

The overall systematic uncertainty is clearly dominated by the error on $Br(D_s \to \phi\pi)$ and by the error on $f_s/f_d$. The measurement of $Br(D_s \to \phi\pi)$ will soon be dramatically improved by Cleo C and the measurement of $f_s/f_d$ is also underway at CDF. With the total systematic error reduced and the statistical error improved the new measurement of $Br(B_s \to D_s\pi)/Br(B^0 \to D\pi)$ can actually be sensitive to isolate the contributions of tree level and non-tree level diagrams.


[1] F. Abe, et al., Nucl. Instrum. Methods Phys. Res. A **271**, 387 (1988); D. Amidei, et al., Nucl. Instum. Methods Phys. Res. A **350**, 73 (1994); F. Abe, et al., Phys. Rev. D **52**, 4784 (1995); P. Azzi, et al., Nucl. Instrum. Methods Phys. Res. A **360**, 137 (1995); The CDFII Detector Technical Design Report, Fermilab-Pub-96/390-E

[2] S. Eidelman *et al.*, Physics Letters **B592**, 1-1110 (2004).

[3] D. Acosta *et al.* [CDF Collaboration], "Measurement of the J/psi meson and b-hadron production cross sections in p anti-p collisions at s**(1/2) = 1960-GeV," Phys. Rev. D **71**, 032001 (2005)

[4] D. Langle, Nucl. Meth. in Phys. Res. **A 462**, (2001) 152-155

[5] P. Nason, S. Dawson and R.K. Ellis, Nucl. Phys. **B303** (1988) 607; Nucl. Phys. **B327** (1989) 49.

[6] C. Peterson *et al.*, Phys. Rev. **D27** (1983) 105.

[7] B. Aubert et al. (Babar Collaboration) " Measurement of $D_s \to \phi\pi$ Branching fraction " Phys.Rev. D71 (2005) 091104

## VII. BLESSED TABLES.

| Branching Ratio | Value |
|---|---|
| $D^+ \to K^-\pi^+\pi^+$ | $9.2 \pm 0.6 \cdot 10^{-2}$ |
| $D_s^+ \to \phi\pi^+$ | $4.81 \pm 0.64 \cdot 10^{-2}$ |
| $\phi \to K^+K^-$ | $49.2 \pm 0.6 \cdot 10^{-2}$ |
| $f_s/f_d$ | $0.259 \pm 0.038$ |

TABLE I: Branching fractions used for calculations of the relative rates of $B$ mesons, as taken from the PDG [2]. $D_s$ Branching fraction comes from the most recent Babar measurement [7].

| Cut | $B^0$ | $B_s$ |
|---|---|---|
| d0 | $< 0.007$ | $< 0.0075$ |
| $\chi^2_{r-\phi}(B)$ | $< 15$ | $< 15$ |
| $\chi^2_{r-\phi}(D)$ | $< 14$ | $< 14$ |
| $L_{xy}/\sigma(B)$ | $> 7.0$ | $> 8.0$ |
| $p_T(\pi_B)$ | $> 1.0$ | $> 1.0$ |
| $L_{xy}(B \leftarrow D)$ | $>$ -0.02 | $>$ -0.02 |

TABLE II: $B^0 \to D^-\pi$ Cuts after cut optimization for `B_CHARM`. In addition to these requirements, when reconstructing $B_s$ mesons, we require that the invariant mass of the two kaon tracks be between 1010 and 1029 MeV/$c^2$.

| Effect | Syst. Uncertainty [%] |
|---|---|
| $B$ $p_T$ spectrum | $\pm1.5$ |
| $\phi^0$ mass cut | $\pm0.5$ |
| cut efficiencies | $\pm0.0$ |
| $B_s$ lifetime | $\pm2.1$ |
| $D_s^+$ lifetime | $\pm0.0$ |
| $B^0$ lifetime | $\pm0.4$ |
| $D^+$ lifetime | $\pm0.0$ |
| $B_s$ fitting | $\pm1.5$ |
| $B^0$ fitting | $\pm0.5$ |
| Total | $\pm3.1$ |

TABLE III: Table of systematic errors for the $B_s/B^0$ relative branching fraction measurements

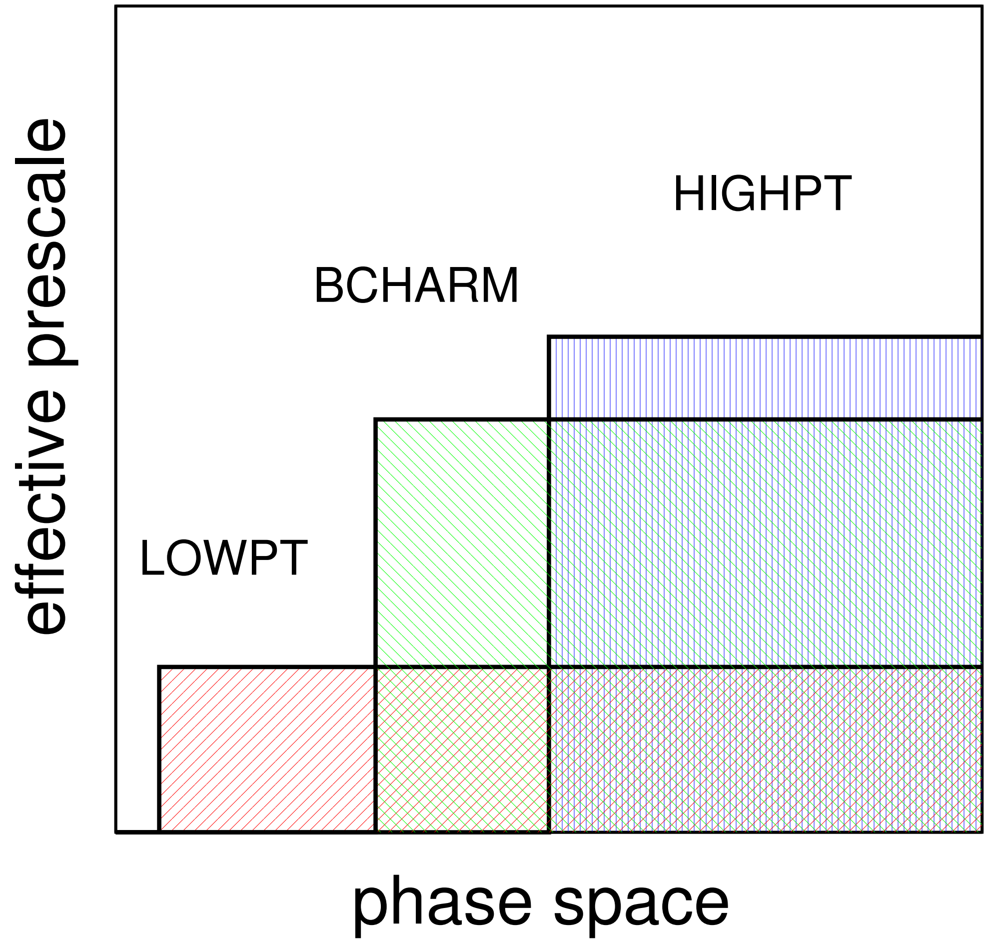


FIG. 1: Three branches of the hadronic trigger. The plot represents the set of selection requirements of the triggers(phase space) versus the effective trigger prescale.

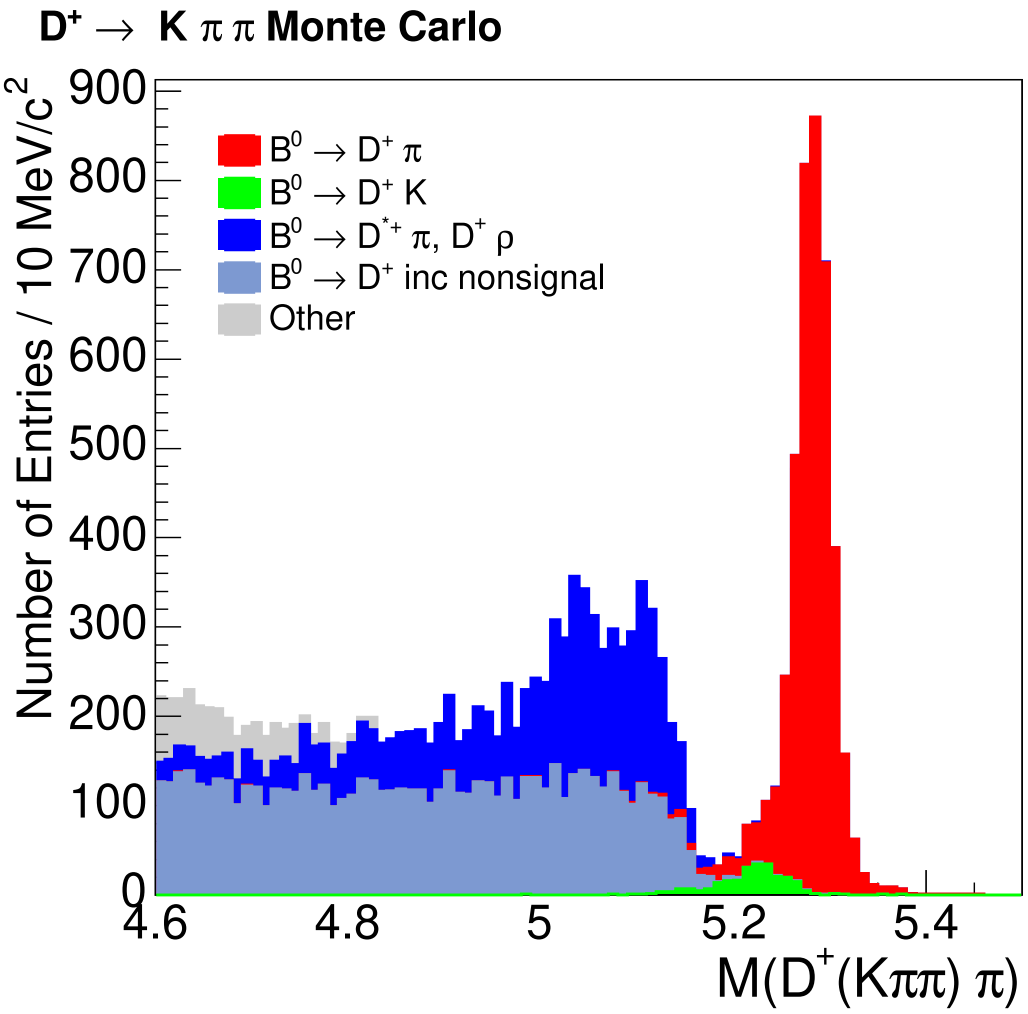


FIG. 2: Decomposition of the single-$B$ background for $B^0$ decays. In the plot, the decomposition is done in such a way to show which decays cause the spiked structure in the mass peak.

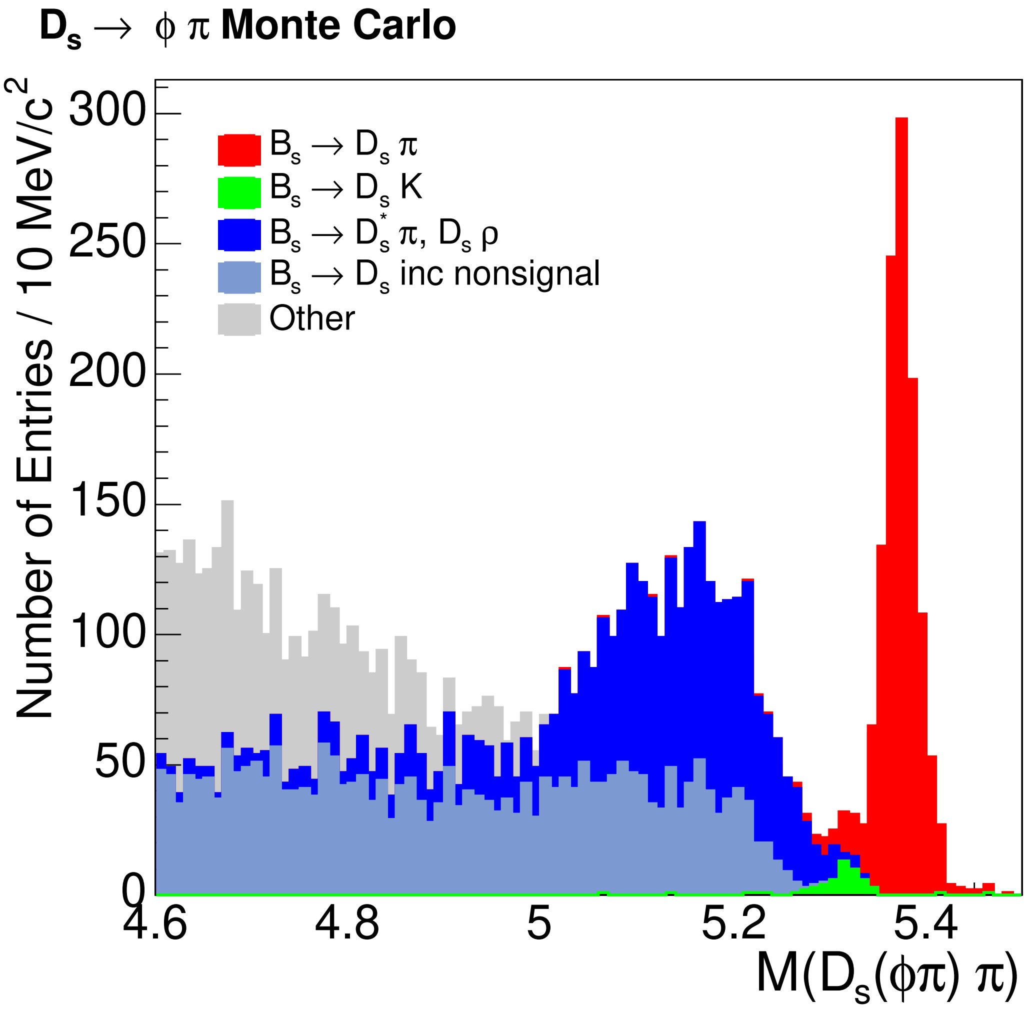


FIG. 3: Decomposition of the single-$B$ background for $B_s$ decays. On the plot, the decomposition is done to show the background in the all of the fitting range.

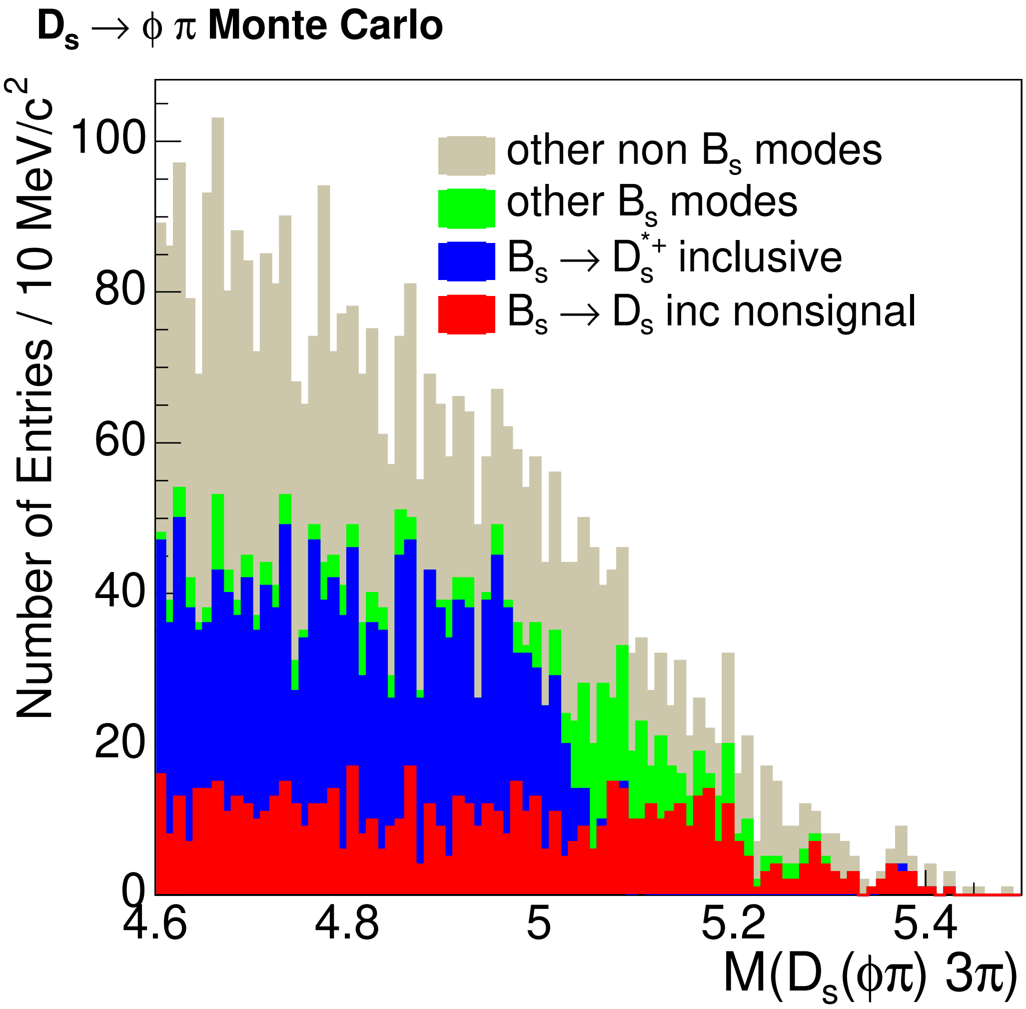


FIG. 4: The plot shoes the breakdown of continuum background for $B_s$ meson in three categories: decays involving $B_s$ decaying to $D_s$(the signal modes being subtracted),decays involving $B_s$ decaying to $D_s^*$(subtracting the main reflection modes and $D_s D_s^*$ mode to avoid double counting) and the "other" category which involves $B^0$, $B^+$ and the other $B_s$ decays.

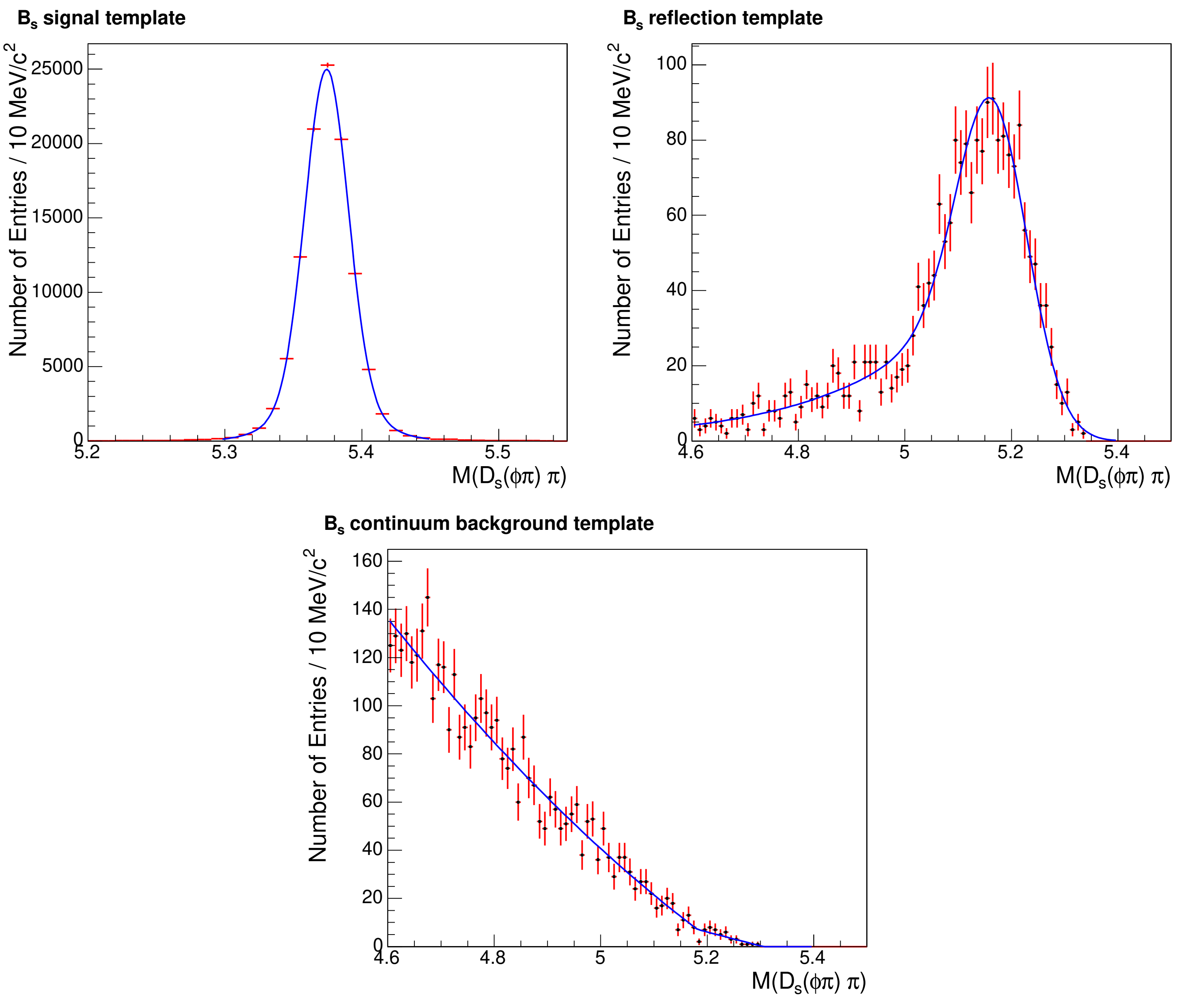


FIG. 5: Templates used in $B_s \to D_s\pi$ fitting for combined B_CHARM and LOWPT trigger data: top left, double Gaussian is used to fit the signal; top right, the structure due to $D_s^*\pi$, $D_s\rho$ decays. The bottom plot shows the distribution from other $D_sX$ decays. The analytical templates used to fit the data are overlaid.

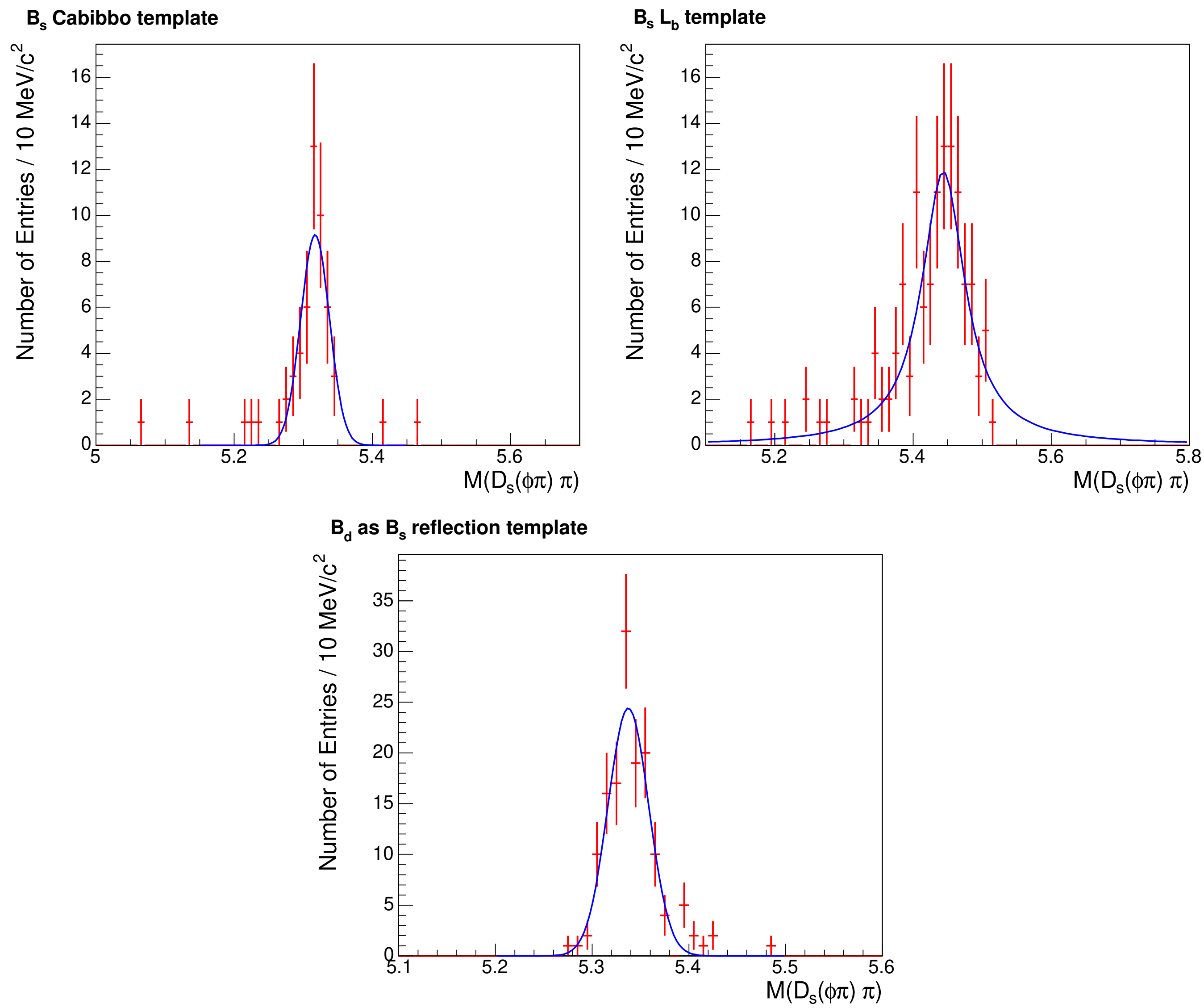


FIG. 6: Templates used in $B_s \to D_s\pi$ fitting for combined B_CHARM and LOWPT trigger data: top left, the template used in the fit of Cabibbo suppressed $B_s \to D_s K$ decay; top right, the template due to $\Lambda_b \to \Lambda_c\pi$ decay. The bottom plot shows the distribution due to$D\pi$ reflection where one pion inside the D candidate is reconstructed as kaon. The analytical templates used to fit the data are overlaid.

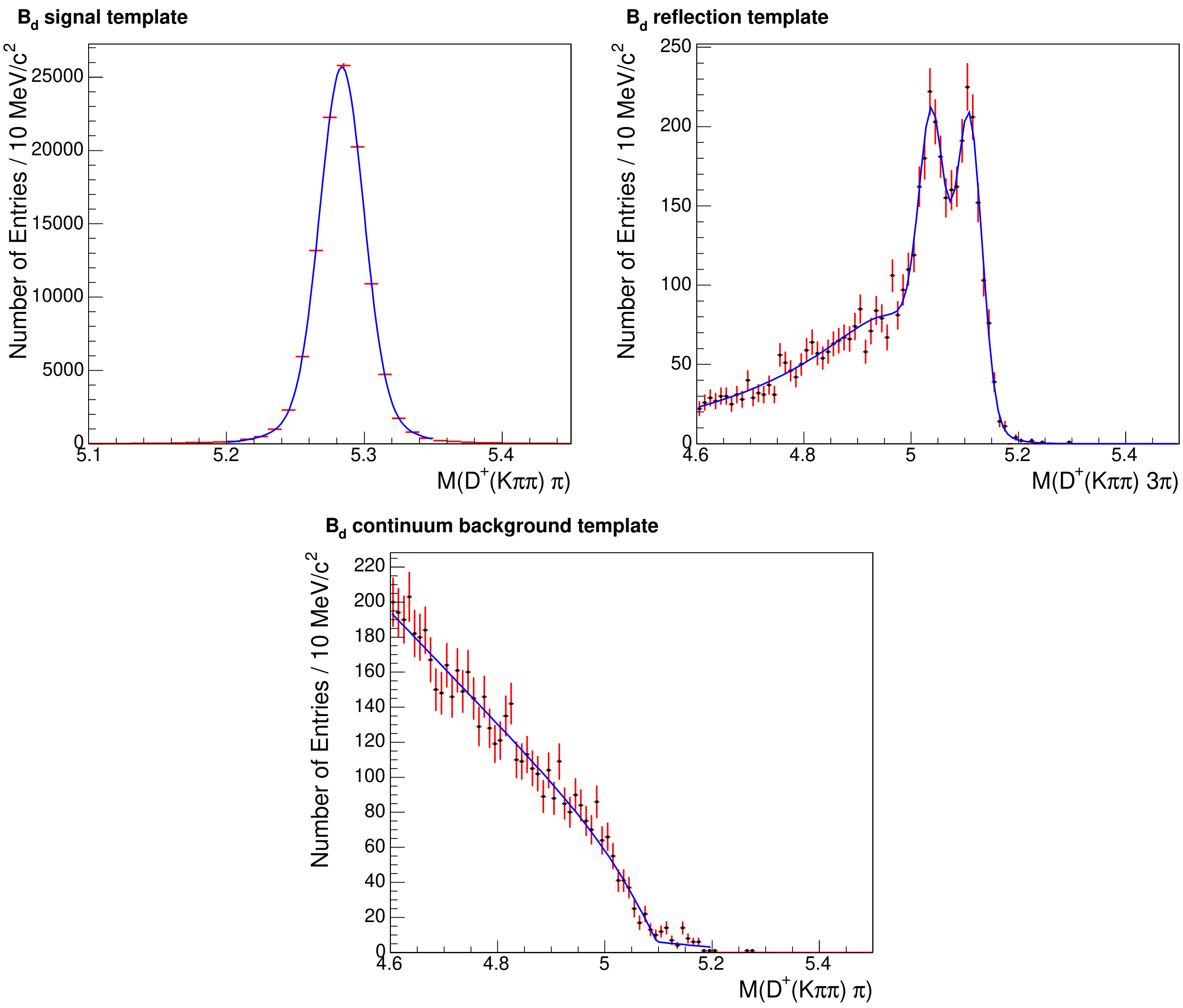


FIG. 7: Templates used in $B^0 \to D\pi$ fitting for combined `B_CHARM` and `LOWPT` trigger data: top left, double Gaussian is used to fit the signal; top right, the structure due to $D^*\pi$, $D\rho$ decays. The bottom plot shows the distribution from other $DX$ decays. The analytical templates used to fit the data are overlaid.

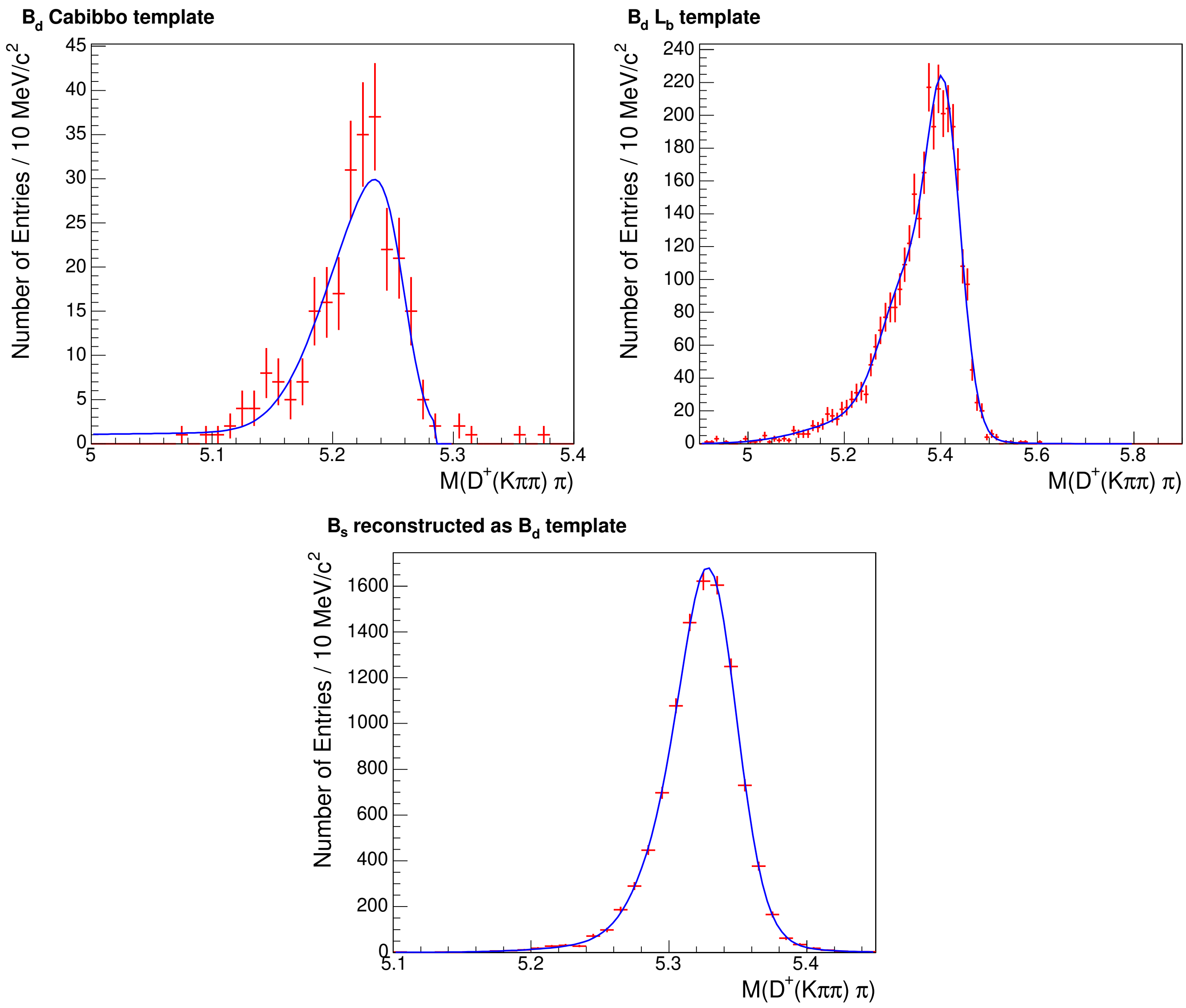


FIG. 8: Templates used in $B^0 \to D\pi$ fitting for combined `B_CHARM` and `LOWPT` trigger data: top left, the template used in the fit of Cabibbo suppressed $B^0 \to DK$ decay; top right, the template due to $\Lambda_b \to \Lambda_c\pi$ decay. The bottom plot shows the distribution due to $D\pi$ reflection where one pion inside the D candidate is reconstructed as kaon. The analytical templates used to fit the data are overlaid.

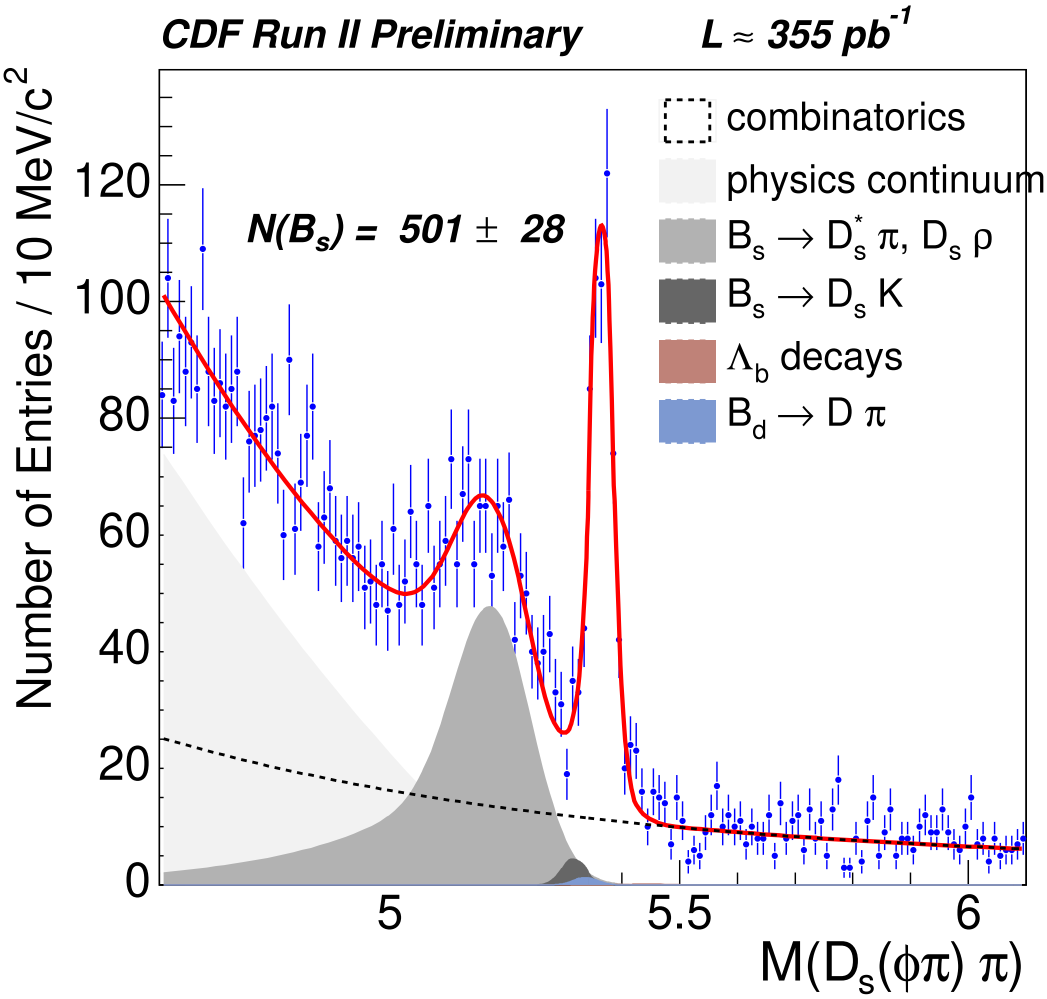


FIG. 9: Mass distribution for $B_s \to D_s\pi^+$ candidates reconstructed with optimized selection requirements for the combined `B_CHARM` and `LOWPT` trigger data. The fit result yields $501 \pm 28$ candidates.

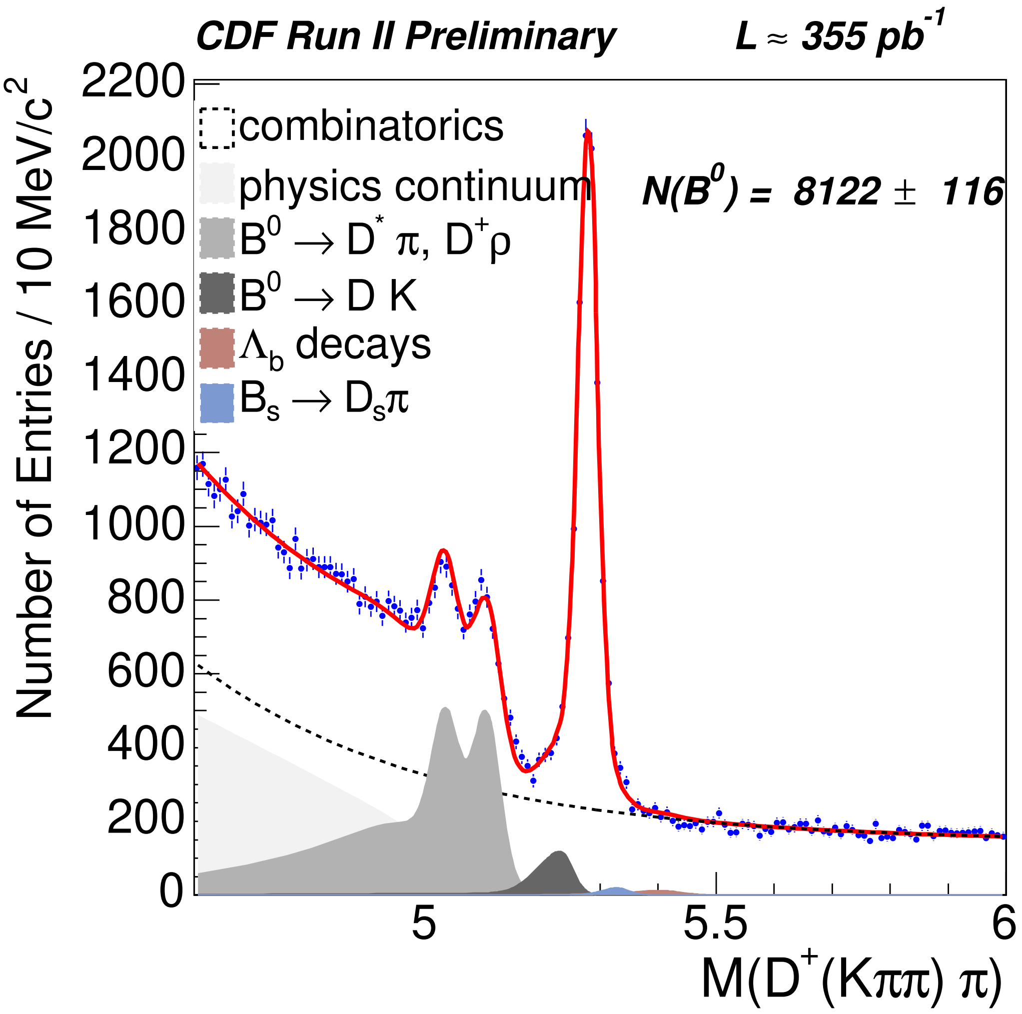


FIG. 10: Invariant mass distribution for $B^0 \to D^-\pi^+$ candidates reconstructed with optimized selection requirements for the combined `B_CHARM` and `LOWPT` trigger data. The fit result yields $8122 \pm 116$.